ELSEVIER

Bioorganic & Medicinal Chemistry Letters

Bioorganic & Medicinal Chemistry Letters Vol. 17, No. 11, 2007

Contents

ARTICLES

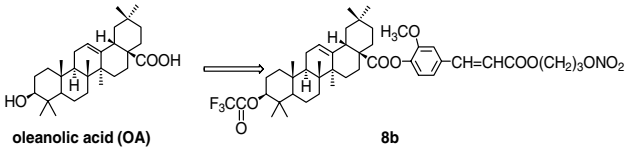

A series of NO-releasing derivatives of OA were synthesized and identified as inhibitors of HepG2 cell apoptosis. The most potent compound **8b** protected hepatocytes from anti-Fas-mediated apoptosis at 10^{-10} M.

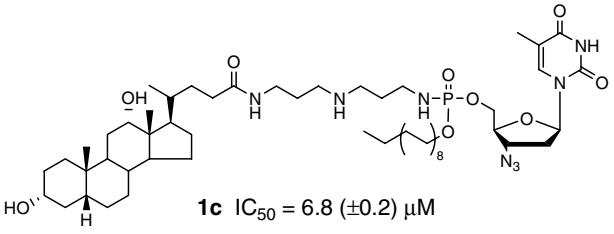

Design, synthesis, and antitumor evaluation of a series of bile acid–polyamine–AZT phosphoramidate conjugates are reported.

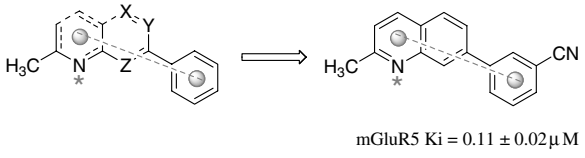

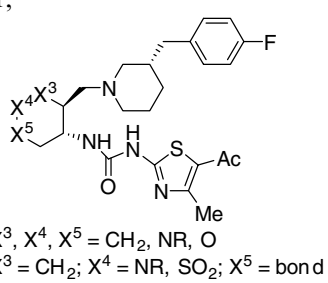

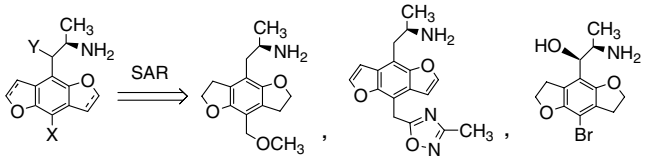

A series of benzodifuran analogs with reduced lipophilicity were designed and synthesized as novel 5-HT$_{2A}$ agonists. The selected compounds **5**, **18**, and **25** exhibited potent and efficacious ocular hypotensive activity in cynomolgus monkey eye, affording maximum IOP reductions of 37%, 27%, and 24%, respectively, at 300 μg doses.

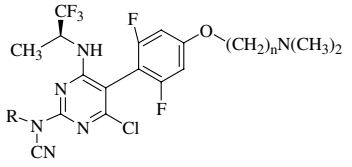

The synthesis, SAR, and mechanism of action studies for a series of 2-cyanoaminopyrimidines as anticancer agents is reported.

4-Substituted phenyl cyclohexanes were identified as alternative isosteres for the biphenyl moiety of the lead compound **1**. The syntheses, SAR optimization, and pharmacokinetic profiles of these compounds are described.

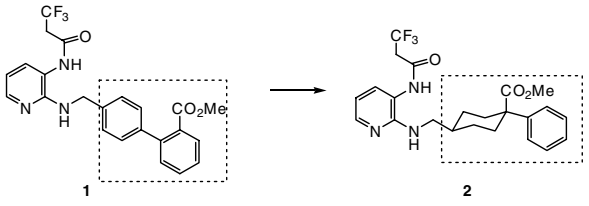

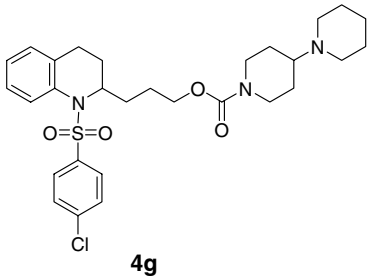

4g
γ-secretase IC_{50} = 60 nM

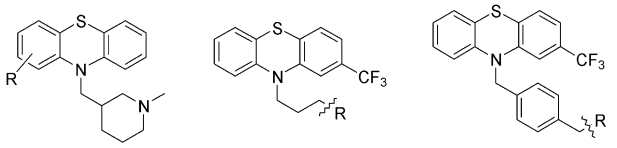

A series of phenothiazines were synthesized and evaluated for activity against *Mycobacterium tuberculosis*. The compounds were subsequently counter-screened for binding to dopamine and serotonin receptors to determine the in vitro selectivity of the compounds for antitubercular activity over psychotropic effects.

The synthesis of novel aminoethylbiphenyls with high affinity for the 5-HT$_7$ receptors and good selectivity towards 5-HT$_{1A}$ receptors is reported.

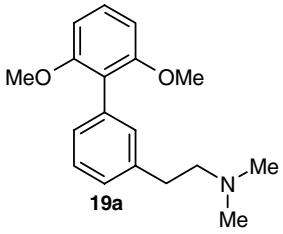

19a

Ki 5-HT$_7$ = 8.6 nM
Ki 5-HT$_{1A}$ = 4826 nM

A series of 4-hydroxy-4-phenylpiperidines have been synthesized and bind to the nociceptin receptor with high affinity. The synthesis and structure–activity relationships at the N-1 and C-4 hydroxy are described.

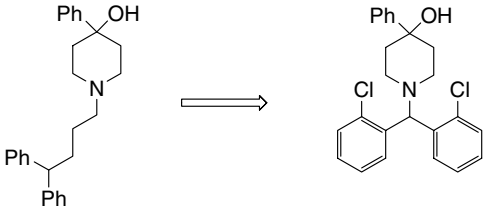

1 NOP K_i= 613 nM

52 NOP K_i= 2 nM

A series of 4-[2-(aminomethyl)phenyl]-1-[bis(2-chlorophenyl)methyl]-4-hydroxypiperidine analogs has been identified as nociceptin receptor ligands. These compounds display high affinity and functional activity at the nociceptin receptor. The synthesis and structure–activity relationships at the C-4 phenyl and N-1 positions are described and the antitussive activity of a selected compound is reported.

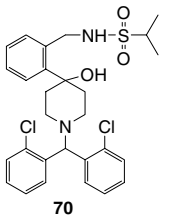

70

Antitussive activity (ED_{50}):
0.06 mg / kg (2 h) ; 0.15 mg/kg (6 h)

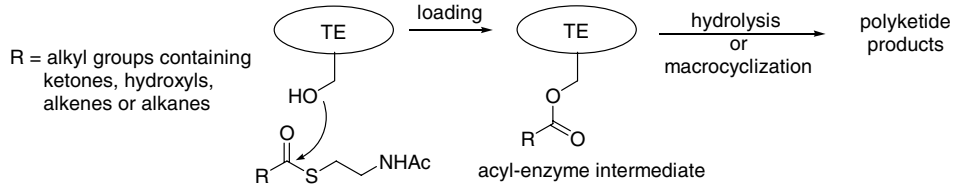

Thioesterase domains exhibit low substrate specificity for loading and can generate the acyl-enzyme intermediates, required for hydrolysis or macrocyclization, from a number of structurally different thioesters.

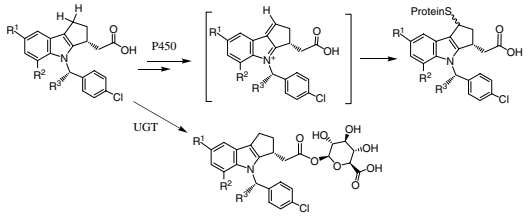

Impacts of substituents on the indole-core of DP1 receptor antagonists on reactive metabolite formation and in vitro and in vivo covalent binding to liver proteins.

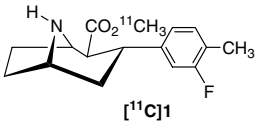

A series of 2β,3α-(substituted phenyl)nortropanes was synthesized and evaluated in vitro for human monoamine transporters. Radiolabeling and nonhuman primate microPET brain imaging studies were performed with the most promising compound, [^{11}C]**1**, to determine its utility as a NET imaging agent.

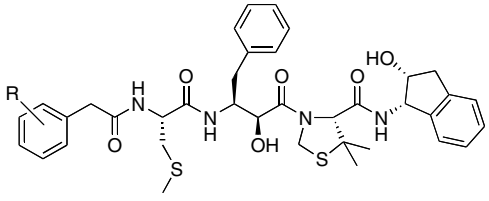

A series of allophenylnorstatine-containing tripeptidic compounds were synthesized with various N-terminal phenylacetyl moieties. Certain derivatives exhibited extremely potent inhibitory activity against plasmepsin II.

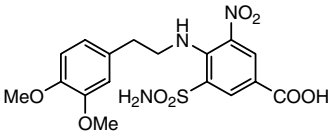

We have identified new lead candidates, which showed inhibition against *Mycobacterium tuberculosis* Chorismate Mutase, by a combination of ligand-based virtual screening and biological assays.

trans-Tiliroside (0.1–10 mg/kg/d) from the seeds of *Rosa canina* potently inhibited the gain of body weight, especially visceral fat weight, and significantly reduced blood glucose levels after loading of glucose (1 g/kg, ip) in mice. On the other hand, kaempferol and *p*-coumaric acid lacked such effect and kaempferol 3-*O*-β-D-glucopyranoside tended to reduce the gain of body weight and visceral fat weight, but not significantly, at a dose of 10 mg/kg/d. These results indicate the importance of both kaempferol 3-*O*-β-D-glucopyranoside and *p*-coumaroyl moieties for anti-obese effects. Furthermore, a single oral administration of *trans*-tiliroside at a dose of 10 mg/kg increased the expression of PPAR-α mRNA of liver tissue in mice.

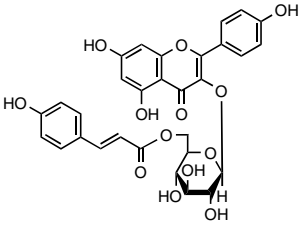

trans-tiliroside

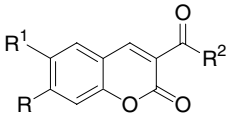

A novel class of selective anti-*Helicobacter pylori* agents, 2-oxo-2*H*-chromene-3-carboxamide derivatives, were prepared and evaluated for their anti-bacterial activity. Some of them exhibited a potent and specific inhibitory effect on the growth of *H. pylori*.

A series of 3-(1*H*-benzo[d]imidazol-2-yl)pyridin-2(1*H*)-one inhibitors of insulin-like growth factor receptor-1 (IGF-1R) were examined in which the pendant imidazole moiety was replaced to improve selectivity for IGF-1R inhibition over cytochrome P450 (CYP). Synthesis and SAR of these compounds is presented.

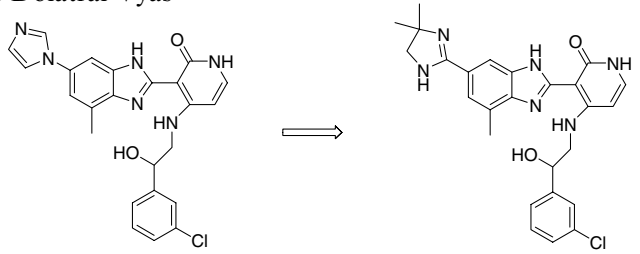

IGF1R IC_{50} = 0.18 μM
CYP3A4 IC_{50} = <0.046 μM

IGF1R IC_{50} = 0.0 46 μM
CYP3A4 IC_{50} = >5.1 μM

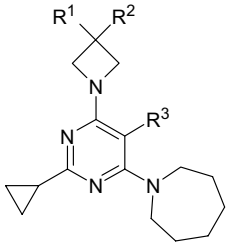

The SAR around 3-substituted azetidinylpyrimidine derivatives as potent dual M_3 antagonists and PDE4 inhibitors is reported.

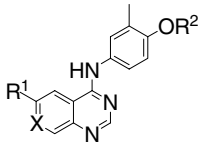

The synthesis and biological evaluation of potent and selective inhibitors of the erbB2 kinase is presented. The vast majority of these compounds are found to be >100× selective over the closely related EGFR kinase. Two lead compounds are further shown to have low clearance and moderate bioavailability in rat.

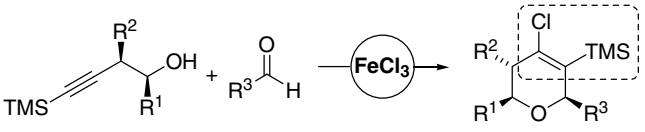

The inexpensive, stable and environmentally friendly $FeCl_3$ promotes the Prins cyclization to synthesize functionalized alkyl chlorodihydropyrans. The method represents an efficient and regioselective manner to obtain in a single step chlorovinyl–TMS oxacycles with enhanced cytotoxicity against human solid tumor cells.

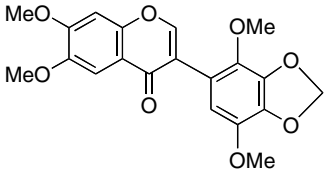

Glaziovianin A (1)

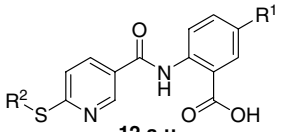

12 a-u

R^1 = CN, Cl, Br

This paper describes the SAR in the anthranilic acids as antibacterial agents against Gram-positive organisms and how that activity relates to the compounds, affinity for human serum albumin (HSA).

Structural modifications of the initial lead, 3-aminochroman (**4**), led to the identification of a novel series of pyridyl-fused amino chroman derivatives (**5**–**8**) and the structural isomers (**9**–**12**). The compounds described were evaluated for dual 5-HT transporter inhibitory and 5-HT_{1A} receptor activities. The design strategy, synthesis, and in vitro biological characterization for these novel compounds are described.

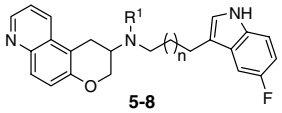

5-8

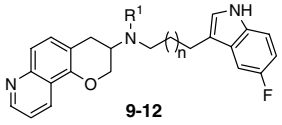

9-12

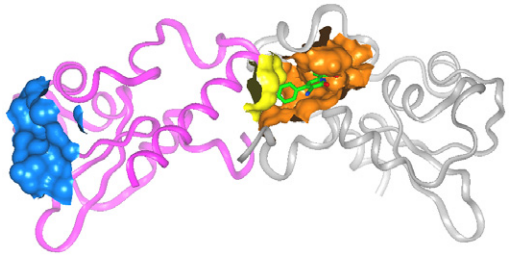

The synthesis and structure–activity relationships of a series of novel phenoxyphenyl diamine derivatives with affinity for both the histamine H_3 receptor and the serotonin transporter is described.

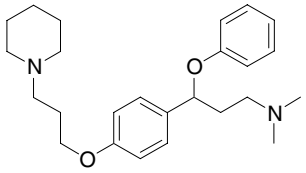

14

hH_3 K_i = 0.6 nM

rSERT K_i = 1.0 nM

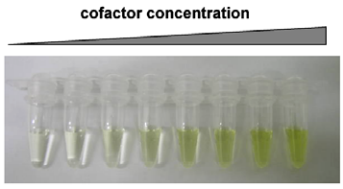

We constructed a label-free and detector-free aptazyme-based riboswitch sensor for detecting the cofactor of the aptazyme.

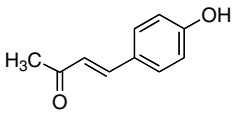

Structure function analysis of benzalacetone synthase from *Rheum palmatum* is reported.

Safrole oxide has no effect on the growth of mouse neural stem cells. But the apoptotic VECs triggered by safrole oxide induced NSC apoptosis in the co-culture system.

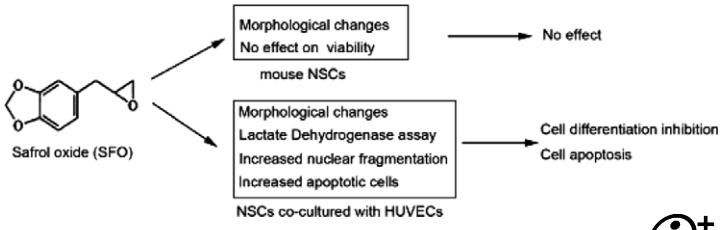

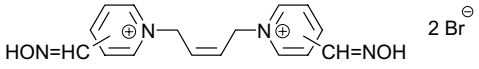

A series of bisquaternary reactivators of acetylcholinesterase (AChE) bearing (*Z*)-but-2-ene connecting linker was synthesized and evaluated on tabun and paraoxon-inhibited AChE with promising results.

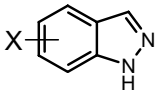

X= Hal, NO_2

The synthesis and in vitro and in vivo pharmacological evaluation of a complete series of substituted indazoles as new inhibitors of nNOS are reported.

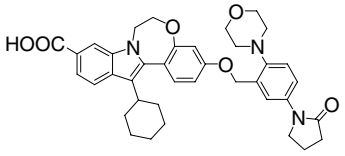

7 EC_{50} = 7.6 nM

Fluorinated substrate analogs were synthesized and incubated with rat liver 3-hydroxyacyl-CoA dehydrogenase, which reveals that the formation of an enolate intermediate is required for the enzymatic reaction.

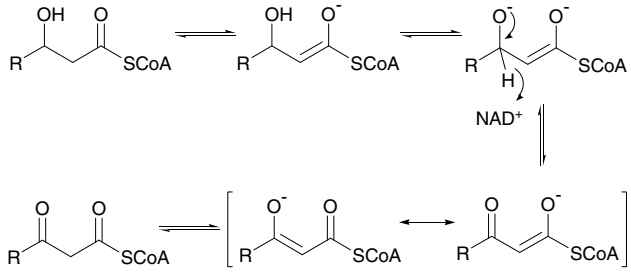

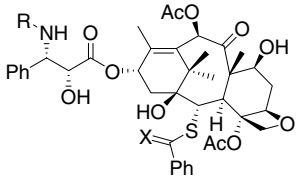

R=Bz, Boc
X=O, H_2

The biotransformation of gentiopicroside by asexual mycelia of *Cordyceps sinensis* yielded two products, one of which was proved to be a new pyridine monoterpene alkaloid. The possible mechanisms were discussed.

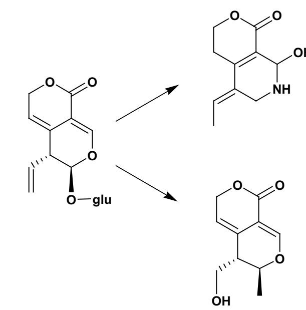

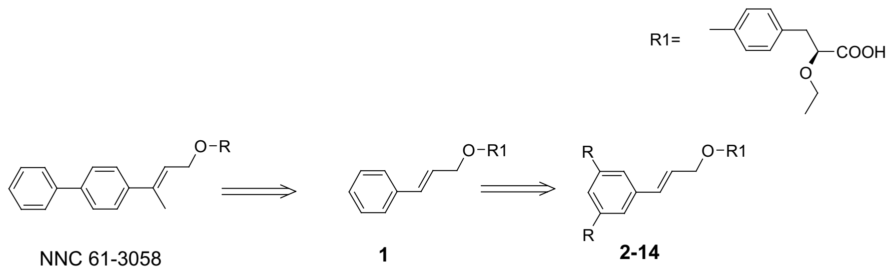

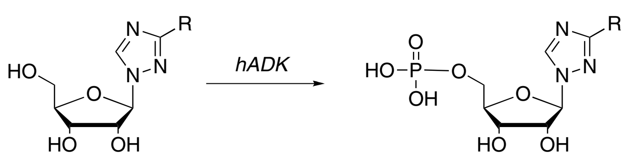

Variation of the 3-substituents in a series of bioisosteric and homologated 1-β-D-ribofuranosyl-1,2,4-triazoles has marked effects on activity with the human adenosine kinase, and analysis of computational descriptors and binding models offers insight for the design of novel substrates.

A novel series of 2-hydroxy-*N*-arylbenzenesulfonamides were identified to be ATP-citrate lyase (ACL) inhibitors with compound **9** displaying potent in vitro activity (IC_{50} = 0.13 μM). Chronic oral dosing of compound **9** in high-fat fed mice lowered plasma cholesterol, triglyceride, and glucose, as well as inhibited weight gain.

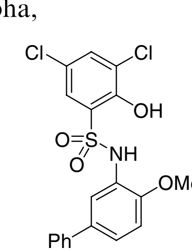

9

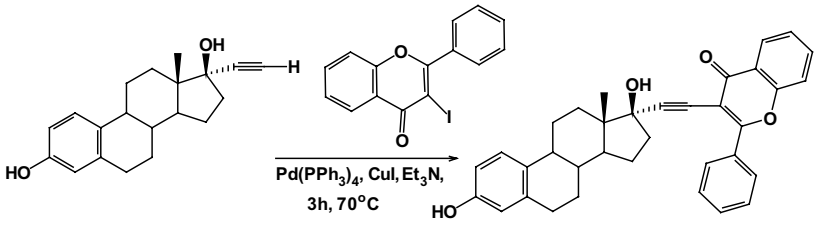

Flavone-, indole-, and furan-17β-estradiol conjugates with 2–8 carbon linker chains extending from the 17α-position of the estradiol were synthesized by Pd-catalyzed cross-coupling reactions. In vitro competitive binding assays for the estrogen receptor revealed that a two-carbon alkynyl linker combined with a flavone conjugate provided the highest binding affinity.

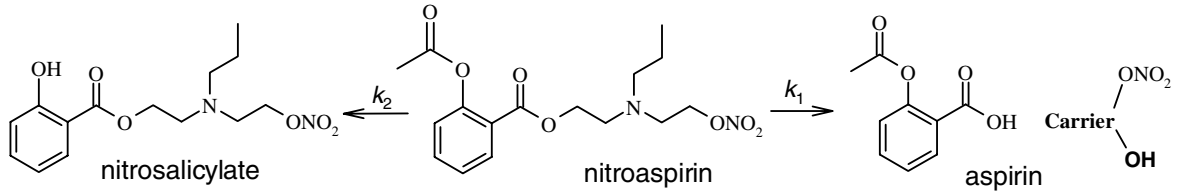

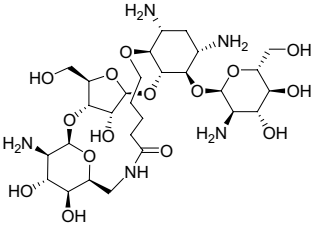

Based on molecular modeling and available X-ray structure data on aminoglycosides complexed with a bacterial ribosomal surrogate or with a kinase, two analogues of paromomycin were prepared by tethering the 6-OH and the 6‴-NH_2 group with a five-carbon bridge. Only one of two possible hydroxyl groups was phosphorylated by the kinase. The application of ring closure metathesis is presented for the first time to construct bridged macrocyclic analogues in the aminoglycoside series.

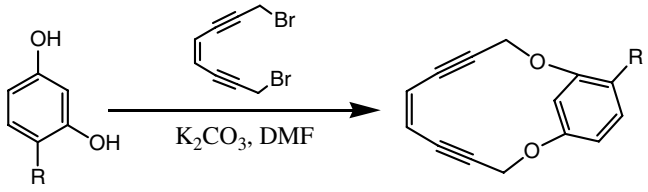

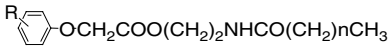

1

The synthesis of the new plant growth regulator **1** is reported.

OTHER CONTENTS

*Corresponding author
ⓘ+ Supplementary data available via ScienceDirect

COVER

Typical snapshot of **7b** bound to HIV-RT from an MC simulation. Carbon atoms of **7b** are gold; from the left, Tyr181, Tyr188, Phe227, Leu100, Lys101; Trp229 at the top, Val106 at the bottom. H-bond with Lys101 O on right. Some residues in front including Glu138 have been removed for clarity. The water on N5 is also H-bonded to a carboxylate O of Glu138. [Thakur, V. T.; Kim, J. T.; Hamilton, A. D.; Bailey, C. M.; Domaoal, R. A.; Wang, L.; Anderson, K. S.; Jorgensen, W. L. *Bioorg. Med. Chem. Lett.* **2006**, *16*, 5664.]

Indexed/Abstracted in: Beilstein, Biochemistry & Biophysics Citation Index, CANCERLIT, Chemical Abstracts, Chemistry Citation Index, Current Awareness in Biological Sciences/BIOBASE, Current Contents: Life Sciences, EMBASE/Excerpta Medica, MEDLINE, PASCAL, Research Alert, Science Citation Index, SciSearch, TOXFILE

ELSEVIER

ISSN 0960-894X